

## Potential changes of the cross section for rectangular microchannel with different aspect ratios

Hyo Song Lee, Ki Ho Kim, Jae Keun Yu, Soon Young Noh, Jae Ho Choi, Soo Kyung Yoon\*, Chang-Soo Lee, Taek-Sung Hwang and Young Woo Rhee†

Department of Chemical and Biological Engineering, Chungnam National University, Daejeon 305-764, Korea

\*Accreditation Board for Engineering Education of Korea, Seoul 135-513, Korea

(Received 30 August 2006 • accepted 18 September 2006)

**Abstract**—In this study, we investigated the potential changes of a rectangular cross section having different aspect ratio and area. A 2D Poisson-Boltzmann equation was used to model the electric double layer field of the cross section. The potential change of the cross section was studied numerically with FEMLAB 3.0 to understand the geometry effects of the rectangular microchannel used for electroosmotic flow. According to the result, the cross-section geometry shows significant influences on the potential field. The potential distribution shows same tendency with various cross-section areas in the same aspect ratio. The potential gradient increases with the increase of the cross section area.

Key words: Electroosmosis, Rectangular Microchannel, Potential, Cross Section

### INTRODUCTION

Microfluidics has been widely studied in the areas using microsystems such as the pharmaceutical-, medical-, bio-, and IT-industries etc., since the microsystems have the benefits of reduced cost, increased reaction intensity, and decreased energy consumption [Manz and Becker, 1998; Stone and Kim, 2001]. Generally, an electroosmotic system consists of two electrodes placed in reservoirs connected with a microchannel. When an external voltage is applied to the electroosmotic system, if the channel wall is negatively charged, positive ions in the solution will be attracted to the wall and make an electric field of the so-called electric double layer (EDL). Then the fluid moves towards the negative electrode, generating an electroosmotic flow (EOF) in that direction [Chun, 2002; Conlisk et al., 2002]. Transporting liquids via an electric field rather than a pressure difference is known as electroosmotic pumping. Electroosmotic pumping has a non-mechanical alternative for the moving of fluid in the microchannel and the flow rate can be easily controlled with external voltage change. Applications of electroosmotic pumping not only include lab-on-a-chip (LOC) devices, but also the pumping of liquids in various micro-electro-mechanical systems (MEMS) [Kou et al., 2004; Gao et al., 2005]. In order to accurately design an electroosmotic system, one must understand the potential change of the cross section in the microchannel [Ren and Li, 2006]. Earlier studies of EDL dealt with simple geometries, such as circular cross section or two parallel plates [Levine et al., 1975]. However, the cross section of recent microchannels is close to a rectangular shape. So the EDL field is to be analyzed with two-dimensions for a rectangular microchannel [Arulanandam and Li, 2000; Li, 2004].

In this paper, we examine the EDL field of a rectangular cross section with various aspect ratios and areas. Aspect ratios (H/W)

are 1, 1/2, and 1/3 and areas are changed from 100 to 900 ( $\mu\text{m}^2$ ). To compare the potential change of the cross section, we made a horizontal line across the center of the cross section and investigated the potential change on that line. A 2D Poisson-Boltzmann equation was used to model the electric double layer field of the cross section and the potential change of the cross section was studied numerically with FEMLAB 3.0 to understand the geometry effects of the rectangular microchannel.

### THEORY

#### 1. Electrical Double Layer Field in a Rectangular Cross Section

Electroosmotic flow depends on the applied electrical field and the local net charge density in the liquid. The local net charge density will depend on the EDL field and the cross section of the microchannel. As shown in Fig. 1, we can consider a rectangular cross section of width 2W and height 2H. The solution domain can be reduced to a quarter section of the cross section since it has symmetry in the potential field.

The 2D EDL field in the rectangular cross section can be described by the Poisson equation of Eq. (1).

$$\frac{\partial^2 \psi}{\partial y^2} + \frac{\partial^2 \psi}{\partial z^2} = -\frac{\rho_e}{\epsilon \epsilon_0} \quad (1)$$

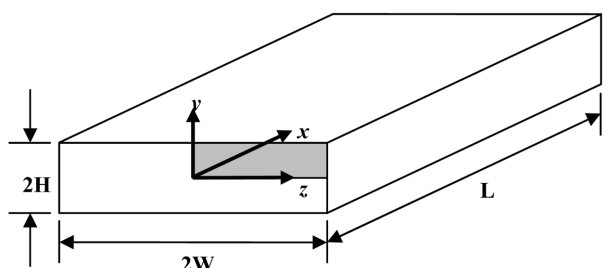


**Fig. 1. Rectangular microchannel with the computational domain (shaded region).**

†To whom correspondence should be addressed.

E-mail: ywrhee@cnu.ac.kr

‡This paper was presented at the 6<sup>th</sup> Korea-China Workshop on Clean Energy Technology held at Busan, Korea, July 4-7, 2006.

where  $\psi$  is the potential,  $\rho_e$  is the net charge density,  $\varepsilon$  and  $\varepsilon_0$  are the dielectric constants in the medium and in the vacuum, respectively. The net charge density for the symmetric electrolyte can be expressed by Boltzmann distribution of Eq. (2).

$$\rho_e = -2n_a z \varepsilon \sinh\left(\frac{ze\psi}{k_b T}\right) \quad (2)$$

Substituting Eq. (2) into Eq. (1), the 2D Poisson-Boltzmann equation is obtained as follows:

$$\frac{\partial^2 \psi}{\partial y^2} + \frac{\partial^2 \psi}{\partial z^2} = \frac{2n_a z \varepsilon}{\varepsilon \varepsilon_0} \sinh\left(\frac{ze\psi}{k_b T}\right) \quad (3)$$

The Poisson-Boltzmann equation can be transformed into non-dimensional equation of Eq. (4) by introducing the dimensionless variables.

$$\frac{\partial^2 \psi^*}{\partial y^{*2}} + \frac{\partial^2 \psi^*}{\partial z^{*2}} = (\kappa D_h) \sinh(\psi^*) \quad (4)$$

where  $y^* = y/D_h$ ,  $z^* = z/D_h$ ,  $\psi^* = ze\psi/k_b T$ ,  $D_h$  is the hydraulic diameter of the rectangular cross section given by Eq. (5), and  $\kappa$  is the Debye-Hückel parameter defined as Eq. (6).

$$D_h = \frac{4A_{cross-sectional}}{P_{wetted}} = \left(\frac{4HW}{H+W}\right) \quad (5)$$

$$\kappa = \left(\frac{2n_a z^2 e^2}{\varepsilon \varepsilon_0 k_b T}\right)^{1/2} \quad (6)$$

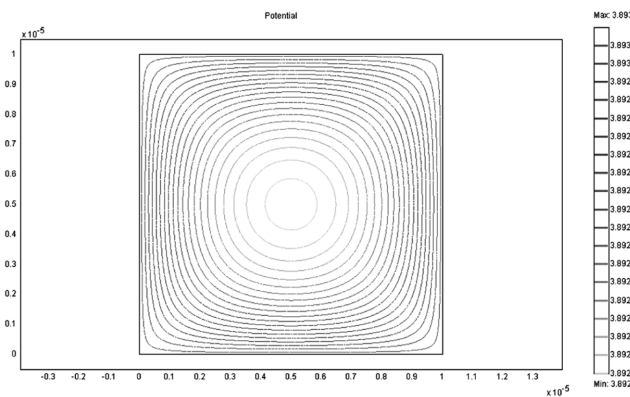
The corresponding non-dimensional boundary conditions are given by:

$$y^* = 0 \quad \frac{\partial \psi^*}{\partial y^*} = 0 \quad (7a)$$

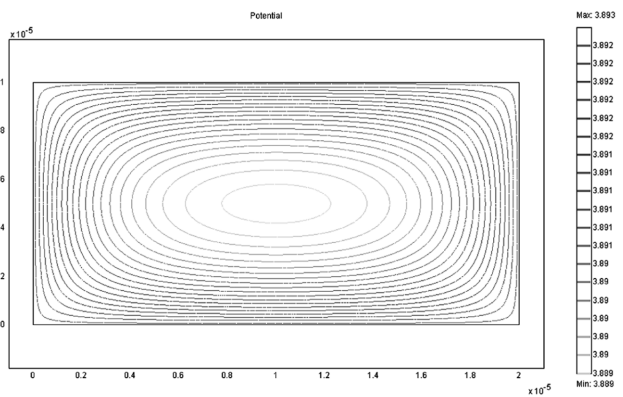
$$z^* = 0 \quad \frac{\partial \psi^*}{\partial z^*} = 0 \quad (7b)$$

**Table 1. Various areas and aspect ratios for potential analysis**

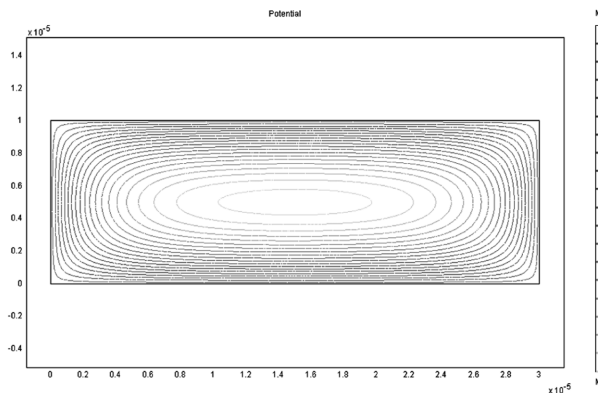
Cross section area ( $\mu\text{m}^2$ )	Height of cross section ( $\mu\text{m}$ )		
	H/W=1	H/W=1/2	H/W=1/3
100	10.00000	7.07107	5.77350
200	14.14214	10.00000	8.16497
300	17.32051	12.24745	10.00000
400	20.00000	14.14214	11.54701
500	22.36068	15.81139	12.90994
600	24.49490	17.32051	14.14214
700	26.45751	18.70829	15.27525
800	28.28427	20.00000	16.32993
900	30.00000	21.21320	17.32051



(a) H/W = 1



(b) H/W = 1/2



(c) H/W = 1/3

**Fig. 2. Contour of the potential in the cross section with different aspect ratio.**

$$y^* = \frac{H}{D_h} \quad \psi^* = \zeta^* = \frac{ze\zeta}{k_b T} \quad (7c)$$

$$z^* = \frac{W}{D_h} \quad \psi^* = \zeta^* = \frac{ze\zeta}{k_b T} \quad (7d)$$

## RESULTS AND DISCUSSION

Various cross section geometries studied numerically with FEM-LAB 3.0 are shown in Table 1. We changed cross section area from 100 to 900 ( $\text{mm}^2$ ) and aspect ratio was changed 1, 1/2, and 1/3 respectively.

The physical properties of KCl aqueous solution were used at a concentration of  $10^{-2}$  M. At room temperature, double layer thickness ( $\kappa^{-1}$ ) can be taken as 3.04 nm. Eq. (4) was applied to the quarter section and then extended to the cross section.

Fig. 2 shows the potential distributions of the cross section having different aspect ratios. As shown in Fig. 2, potential is higher in the nearer area of the boundary, which indicates that the counter ions are concentrated on the channel surfaces. In case where the aspect ratio is 1, potential contour of the cross section shows the circle in the center, which means that the all boundaries have same affection in the cross section. However, as the decrease of the aspect ratio, the circle changes its shape to an ellipse. This result says that the effects of the right side and left side boundaries are decreased and limited to some ranges.

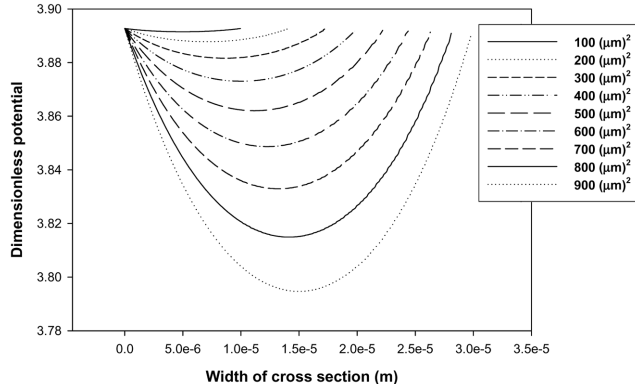


Fig. 3. Potential profile with various cross section areas (H/W=1, zeta potential=0.1 V).

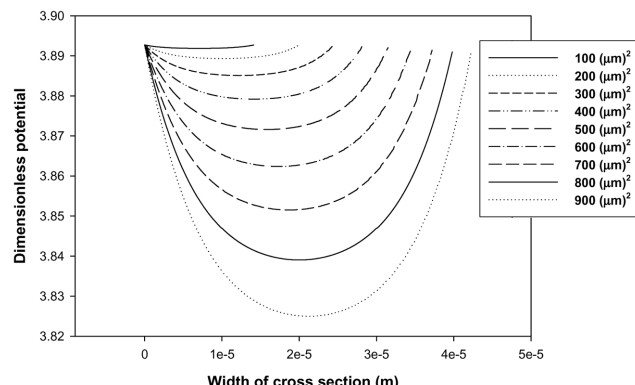


Fig. 4. Potential profile with various cross section areas (H/W=1/2, zeta potential=0.1 V).

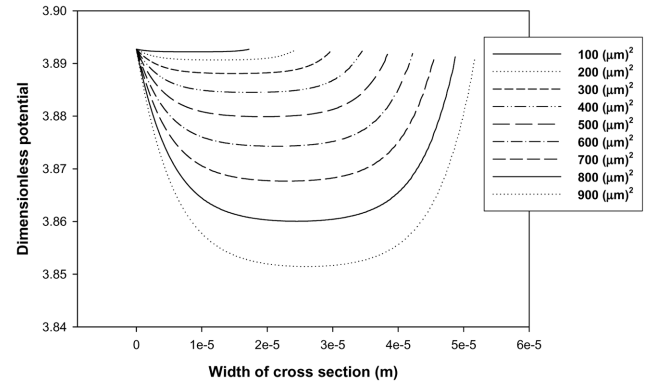


Fig. 5. Potential profile with various cross section areas (H/W=1/3, zeta potential=0.1 V).

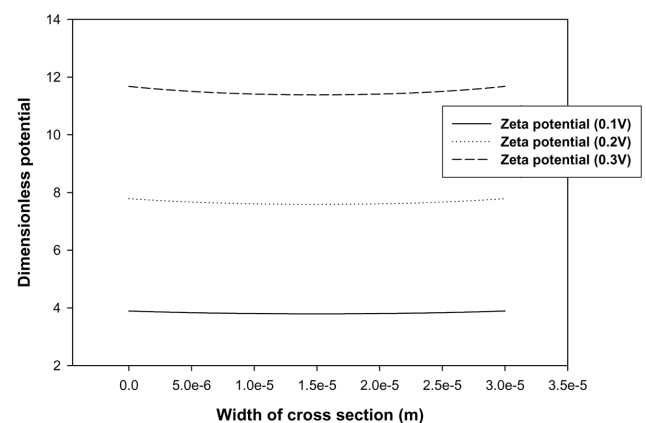


Fig. 6. Potential change with different zeta potentials (H/W=1, area =  $900 \mu\text{m}^2$ ).

In Figs. 3-5, the potential profiles on the horizontal line acrossing the center of cross section are plotted with variations of cross section area. For each aspect ratio, potential profiles have the same shape in every different area, while the lower potential value is decreased with the increase of the cross section area. So the potential gradient increases with the cross section area increase.

The potential change of the cross section with different zeta potentials is demonstrated in Fig. 6, where the aspect ratio is 1 and the area is  $900 \mu\text{m}^2$ . Potential increase is proportional to the increase of zeta potential. This implies that the zeta potential change is a simple method to control the potential of the cross section. The potential changes of other aspect ratios and areas show the same results.

From the potential profiles with different aspect ratios, we chose the potential profiles of the same cross section area and then compared it. Fig. 7 shows the potential variation in the same cross section area with different aspect ratio. As shown in Fig. 7, their shapes are quite different. In case of the aspect ratio is 1, potential gradient is higher than the others and the shape is sharp. In case of the aspect ratio is 1/3, potential gradient exists in some distance and converges to special value. This result indicates that the aspect ratio decrease in the same cross section area could change the potential profile more flatter through the cross section. However, it is difficult to exactly expect the effect of the aspect ratio change in the same cross section area on the flow rate change in the rectangular micro-

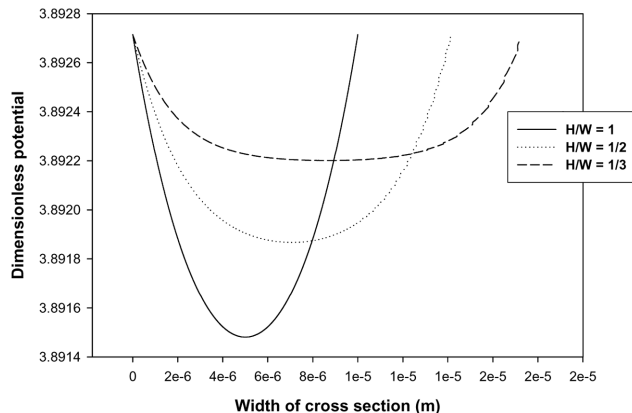


Fig. 7. Potential variation in the same cross section area (zeta potential=0.1 V, area=100  $\mu\text{m}^2$ ).

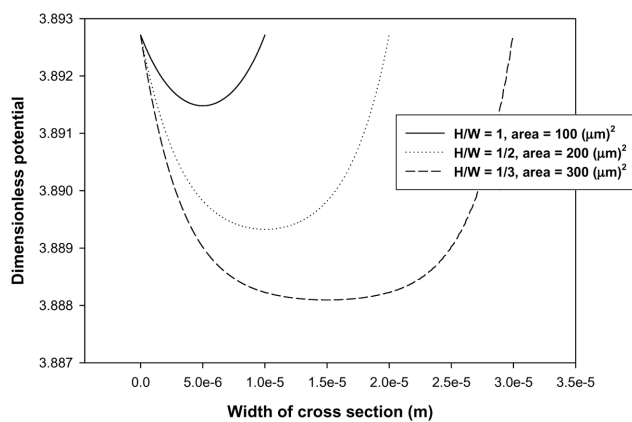


Fig. 8. Potential variation in the same cross section height (zeta potential=0.1 V, height=10  $\mu\text{m}$ ).

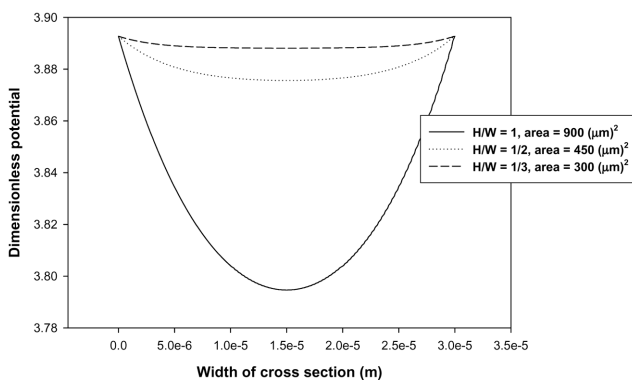


Fig. 9. Potential variation in the same cross section width (zeta potential=0.1 V, width=30  $\mu\text{m}$ ).

channel.

To investigate the effect of the width increase, we compared the potential profiles of the same cross section height. Fig. 8 shows the potential variation in the same cross section height with different aspect ratio. As shown in Fig. 8, the potential gradient is lower in the aspect ratio of 1 and higher in the aspect ratio of 1/3. This result says that increasing the cross section width in the fixed height could

increase the potential gradient. The potential gradient increase means the EDL compression and the zeta-potential increase. So we could increase the electroosmotic flow rate by increasing of the cross section width since it has the effect of the zeta-potential increase.

After investigating the effect of the width increase, we considered the effect of the height increase. As shown in Fig. 9, the potential gradient is lower in the aspect ratio of 1/3 and higher in the aspect ratio of 1. This result implies that increasing the cross section height could increase the potential gradient. As mentioned earlier, the increase of potential gradient could cause the effect of the zeta-potential increase.

Through a comparison of the width change and height change of the cross section, there's no coincidence between the aspect ratio change and potential gradient change, while the cross section area change shows the same tendency with the change of the potential gradient. As a result, we could conclude that increasing the cross section area increases the potential gradient, and then it causes the effect of zeta-potential increase, and finally could increase the electroosmotic flow rate in the microchannel.

## CONCLUSION

The potential profiles of a rectangular cross section were investigated with various aspect ratios and areas. A 2D Poisson-Boltzmann equation was used to model the electric double layer field of the cross section and the potential change of the cross section was studied numerically with FEMLAB 3.0. The potential profiles show the same shape in the same aspect ratio. There's no coincidence between the potential gradient change and the aspect ratio change, while the potential gradient increases with the increase of the cross section area. The potential gradient increase could cause the effect of the zeta-potential increase, and finally could increase the electroosmotic flow rate in the microchannel.

## ACKNOWLEDGMENT

This work is supported by the Korea Science and Engineering Foundation (KOSEF: R01-2003-000-10224-0).

## NOMENCLATURE

$D_h$	: hydraulic diameter [m]
$e$	: elementary charge [C]
$H$	: half channel height [m]
$k_b$	: Boltzmann constant [J/K]
$L$	: channel length [m]
$n_\infty$	: concentration of charged ions [1/m <sup>3</sup> ]
$T$	: temperature [K]
$W$	: half channel width [m]
$Y^*$	: non-dimensional y-coordinate
$z$	: valence of ion
$Z^*$	: non-dimensional z-coordinate

## Greek Letters

$\epsilon$	: dielectric constant in the medium [C <sup>2</sup> /J*m]
$\epsilon_0$	: dielectric constant in the vacuum [C <sup>2</sup> /J*m]

$\rho_o$  : net charge density [ $\text{C}/\text{m}^3$ ]  
 $\psi$  : potential [V]  
 $\psi^*$  : dimensionless potential

## REFERENCES

Arulanandam, S. and Li, D., "Liquid transport in rectangular microchannels by electroosmotic pumping," *Colloids and Surfaces A*, **161**, 89 (2000).

Chun, M. S., "Electrokinetic flow velocity in charged slit-like microfluidic channels with linearized poisson-boltzmann field," *Korean J. Chem. Eng.*, **19**, 729 (2002).

Conlisk, A. T., McFerran, J., Zheng, Z. and Hansford, D., "Mass transfer and flow in electrically charged micro- and nanochannels," *Analytical Chemistry*, **74**, 2139 (2002).

Gao, Y., Wong, T. N., Yang, C. and Ooi, K. T., "Two-fluid electroosmotic flow in microchannels," *J. Colloid Interface Sci.*, **284**, 306 (2005).

Kou, Q., Yesilyurt, I., Studer, V., Belotti, M., Cambril, E. and Chen, Y., "On-chip optical components and microfluidic systems," *Microelectromechanical Engineering*, **73**, 876 (2004).

Levine, S., Mrriott, J. R., Neale, G and Epstein, N., "Theory of electrokinetic flow in fine cylindrical capillaries at high zeta-potentials," *J. Colloid Interface Sci.*, **52**, 136 (1975).

Li, D., *Electrokinetics in Microfluidics*, Elsevier (2004).

Manz, A. and Becker, H., *Microsystem Technology in Chemistry and Life Science*, Springer (1998).

Ren, C. L. and Li, D., "Electrokinetic sample transport in a microchannel with spatial electrical conductivity gradients," *J. Colloid Interface Sci.*, **294**, 482 (2006).

Stone, H. A. and Kim, S., "Microfluidics: basic issues, applications, and challenges," *AICHE*, **47**, 1250 (2001).